Electronic Supplementary Information (ESI) for Chemical Communications
This journal is © The Royal Society of Chemistry 2020

Supporting Information

Synergistically enhanced hydrogen evolution reaction by ruthenium nanoparticles dispersed on N-doped carbon hollow nanospheres

Ji-Sen Li,[a,*] Meng-Jie Huang,[a] Xiao-Nan Chen,[a] Ling-Xin Kong,[a] Yu-Wei Zhou,[a] Ming-Yu Wang,[a] Jun-Lei Li,[a] Ze-Xing Wu,[b] and Xiu-Feng Xu[c]

[a]Department of Chemistry and Chemical Engineering, Jining University, Qufu 273155, P. R. China

[b]State Key Laboratory Base of Eco-chemical Engineering, College of Chemistry and Molecular Engineering, Qingdao University of Science & Technology, Qingdao 266042, P. R. China

[c]School of Chemistry and Chemical Engineering, Institute of Applied Catalysis, Yantai University, Yantai 264005, P. R. China

E-mail: senjili@sina.com

Experimental section

Chemicals

$RuCl_3 \cdot xH_2O$ (M: 225.44) and tetraethyl orthosilicate (TEOS) were obtained from Shanghai Macklin Biochemical Co., Ltd. Poly (sodium 4-styrenesulfonate) (PSS; M_w < 700000 Da) and poly (diallyldimethylammonium chloride) (PDDA; M_w < 500000 Da) were purchased from Alfa Aesar Co. Ltd. Commercial 20% Pt-C was bought from Johnson Matthey. All reagents were utilized without further treatment.

Synthesis of samples

SiO_2@PSS. To prepare the SiO_2@PSS composite, SiO_2 nanospheres were first prepared by modified stöber approach and selected as hard templates to control the entire morphology throughout the overall synthetic process. Namely, ethanol (100 mL), H_2O (6 mL), ammonium hydroxide (6 mL), and TEOS (3 mL) were gradually added together and mechanically stirred for 5 h, then the products were separated by centrifugation at 10000 rpm for 5 min, and washed several times with water and ethanol. Finally, the solid was dried at 80 ^oC for 6 h under vacuum to obtain SiO_2 nanospheres. The resulting SiO_2 nanospheres were coated with negative charges according to a self-assembly strategy. In brief, 500 mg of the as-prepared SiO_2 nanospheres were added into 100 mL of NaCl solution (0.5 M) and sonicated for 1 h. After the addition of PDDA (750 mg), the suspension was stirred continuously for 1 h and then separated by centrifugation at 8000 rpm for 7 min, washed three times by H_2O. Subsequently, the obtained sample was dispersed into 100 mL of NaCl solution (0.5 M) and sonicated for 1 h. Then, 0.15 g PSS was added into the above solution and stirred continuously for 1 h. After that, the excess PSS was removed by three repeated centrifugation/wash cycles. By means of repeating the abovementioned method, the as-formed nanospheres were decorated sequentially with PDDA, and PSS to obtain nanospheres with negative charges (denoted as SiO_2@PSS).

Ru@NCHNSs. In a typical procedure, 300 mg of the SiO_2@PSS nanospheres were well-dispersed into 10 mL of water by sonicating for 30 min. Then, 3.3 mL of $RuCl_3$ solution (30 mg mL^{-1}) was added and kept stirring for 4 h. Afterward, 155 mg of histidine was introduced, further stirring for 5 h. The resultant suspension was collected and dried in

a vacuum oven at 90 ^{o}C (SiO_2@$RuCl_3$-His). Next, the as-prepared sample was carbonized at different temperatures (700, 800, and 900 ^{o}C) under the Ar atmosphere for 4 h (SiO_2@Ru@NCNSs-T, T = 700, 800, and 900), respectively. After heating treatment, the product was etched by HF solution to remove the SiO_2 templates, further yielding hollow carbon nanospheres (designed as Ru@NCHNSs).

Ru@NC. The Ru@NC catalyst was also synthesized through the identical procedure except that the SiO_2 nanospheres were not been added.

NCHNSs. The NCHNSs sample was also prepared by the similar method without adding $RuCl_3$.

Instruments

The morphologies and structural features were examined by scanning electron microscope images (SEM, JSM-7600F) at an acceleration voltage of 10 kV and high-resolution transmission electron microscopy (HRTEM, JEM-2100F) at an accelerating voltage of 200 kV. The energy-dispersive X-ray spectroscopy (EDX) was taken on JSM-5160LV-Vantage typed energy spectrometer. To determine the chemical composition of the as-synthesized catalysts, the inductively coupled plasma atomic emission spectroscopy (ICP-AES) were carried out on a Prodigy Leeman ICP-AES spectrometer. The powder X-Ray diffraction (XRD) patterns were recorded on a D/max 2500VL/PC diffractometer (Japan) equipped with graphite monochromatized Cu Kα radiation (λ = 1.54060 Å). Corresponding work voltage and current is 40 kV and 100 mA, respectively. X-ray photon spectroscopy (XPS) was recorded by a scanning X-ray microprobe (PHI 5000 Verasa, ULAC-PHI, Inc.) using Al kα radiation and the C1s peak at 284.8 eV as internal standard. The nitrogen adsorption-desorption experiments were operated at 77 K on a Micromeritics ASAP 2050 system. The pore size distributions were measured by Barret-Joyner-Halenda (BJH) model. Prior to the measurement, the samples were degassed at 150 ^{o}C for 10 h.

Electrochemical Measurements

Electrochemical tests were assessed in a N_2-saturated 1.0 M KOH solution using a three-electrode system. A glassy carbon electrode (GCE, 3 mm in diameter), saturated

calomel electrode (SCE) and a graphite rod were chosen as the working electrode, reference electrode and the counter electrode, respectively. 4 mg of the catalyst was well-dispersed in 1.8 mL of ethanol and 0.2 mL Nafion by ultrasonic for 30 min. Then, 5 μL of the uniform ink was decorated on a glassy carbon electrode as the working electrode, further drying at 40 ^{o}C. The mass loading on the glassy carbon electrode is 0.142 mg cm^{-2}. Linear sweep voltammetry (LSV) was collected at a scan rate of 2 mV s^{-1} with 95% *iR* drop compensation. All of these potentials were calibrated relative to reversible hydrogen electrode (RHE) after transformation ($E_{RHE} = E_{SCE} + 0.059\ pH + E^{\theta}_{SCE}$. In 1.0 M KOH solution, $E_{RHE} = E_{SCE} + 1.0698$.). Electrochemical active surface area (ECSA) was measured by the cyclic voltammogram (CV) curves with in the region of 0.1198-0.2198 V vs. RHE at various scan rates (20-200 mV s^{-1}). The electrochemical impedance spectra (EIS) methods were evaluated in the range of 1000 kHz-0.1 Hz with an amplitude of 10 mV.

The study for full water splitting was investigated with a two-electrode system in 1.0 M KOH solution. The applied voltage window was from 0 to 2.0 V. Each catalyst (2 mg, Ru@NCHNSs, Ru@NC, or commercial 20% Pt-C) was added into 1 mL of ethanol/Nafion mixture solution (v:v = 9:1) and sonicated for at least 30 min, respectively. Subsequently, the ink was coated on the surface of a Ni foam (1 ×1 cm^2), which functioned as the cathode electrode. In parallel, the anode electrode was designed by the same method using commercial IrO_2 as catalyst.

The mass activity (mA mg^{-1}) values of different samples were calculated from the electrocatalyst loading *m* (0.01 mg).

$$j_{mass\ activity}\ (m\text{A mg}^{-1}) = \frac{I\ (m\text{A})}{m\ (m\text{g})}$$

Where,

I (mA) = the measured current

m (mg) = the electrocatalyst loading (0.01 mg)

S1. Figures in Supporting Information

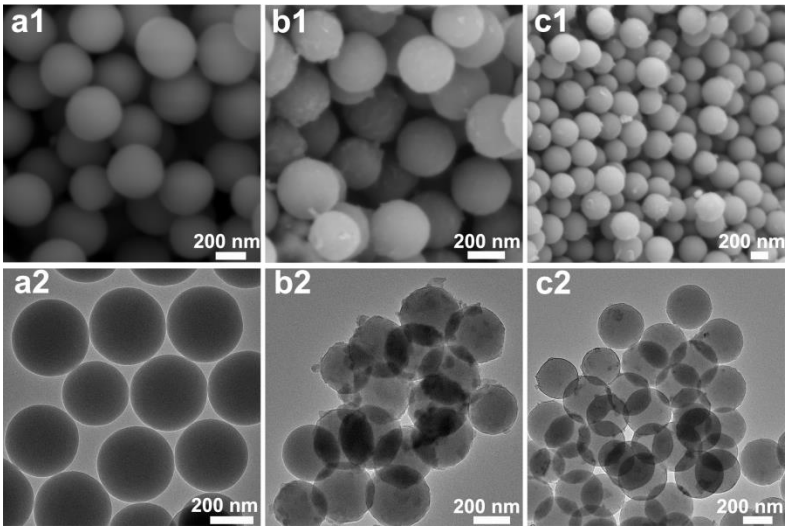

Fig. S1 SEM and TEM images of SiO_2 NSs (a1, a2), SiO_2@$RuCl_3$-His NSs (b1, b2), and SiO_2@Ru@NCNSs (c1, c2).

First, PSS is coated on the surface of the as-prepared SiO_2 nanospheres through a self-assembly approach to fabricate negatively charged SiO_2@PSS nanospheres. Next, the SiO_2@PSS nanospheres are successively wrapped with Ru^{3+} and histidine, denoted as SiO_2@$RuCl_3$-His. Then, the SiO_2@$RuCl_3$-His nanospheres are converted into SiO_2@Ru@NCNSs nanospheres during heating treatment. Last, the SiO_2 template can be selectively etched with HF solution to achieve hollow NCHNSs-anchored Ru NPs nanocomposite. Scanning electron microscope (SEM) image (Fig. S1a) reveals that the SiO_2 nanospheres synthesized by a modified stöber method are greatly homogeneous with a mean size of ~ 380 nm, proven by the corresponding transmission electron microscope (TEM) image (Fig. S1b). Through strong electrostatic attractions, Ru^{3+} ions are adsorbed onto the negatively charged SiO_2@PSS nanospheres. Then, histidine molecules can combine with the Ru^{3+} ions by means of coordination actions. The SEM and TEM images of SiO_2@$RuCl_3$-His show that spherical structure is perfectly retained but the

corresponding surface of the as-formed nanospheres becomes slightly rough (Fig. S1b). After annealing at 800 ^{o}C, the His coating is transformed into N-doped carbon nanospheres, while the Ru^{3+} ions are in situ reduced to ultrafine Ru NPs, yielding the SiO_2@Ru@NCNSs nanocomposite. As displayed in Fig. S1c, it is obviously seen that the sphere-like shape is well preserved without visible change in morphology. Finally, the SiO_2 cores are completely etched by HF solution, further leading to the production of highly dispersed Ru NPs anchored on 3D N-doped carbon hollow nanospheres.

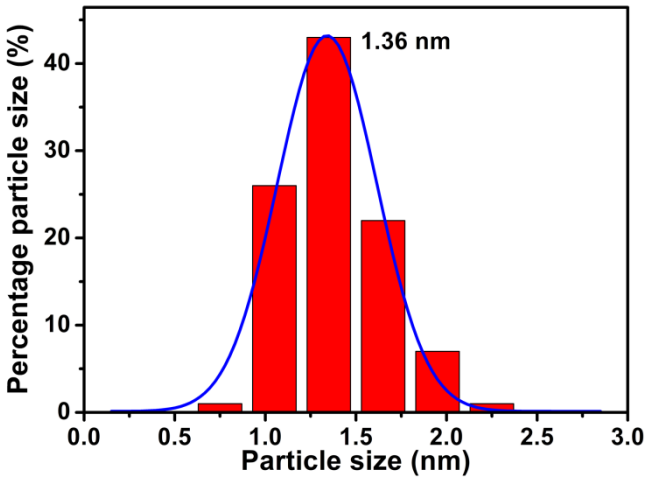

Fig. S2 The particle-size histogram of Ru@NCHNSs.

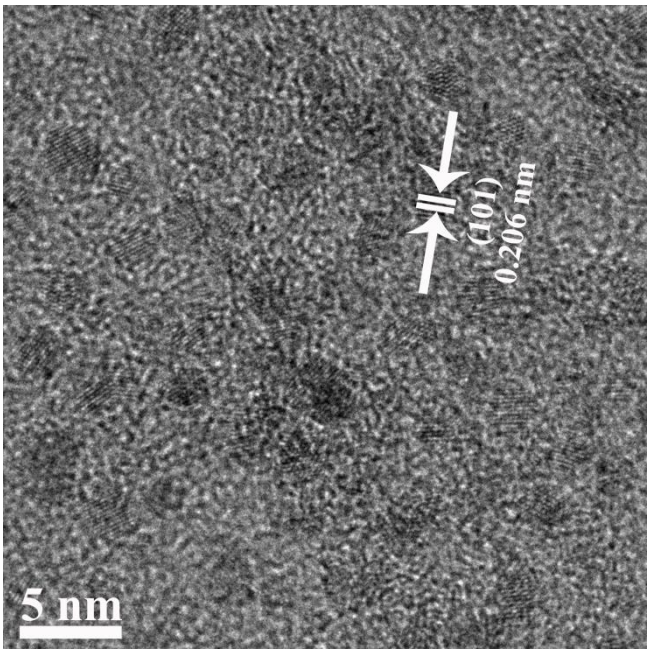

Fig. S3 HRTEM image of Ru@NCHNSs.

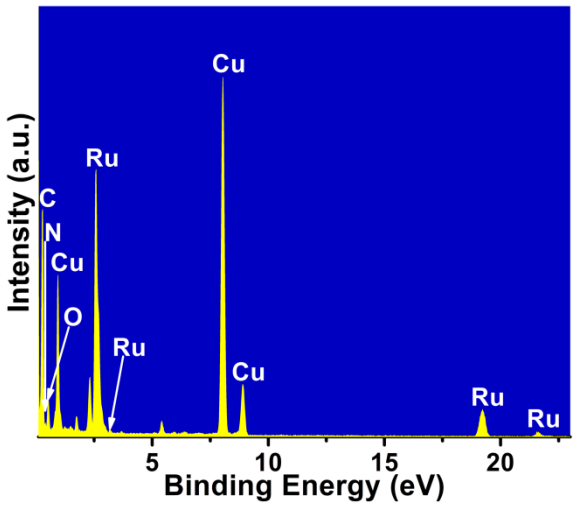

Fig. S4 EDX spectra of Ru@NCHNSs.

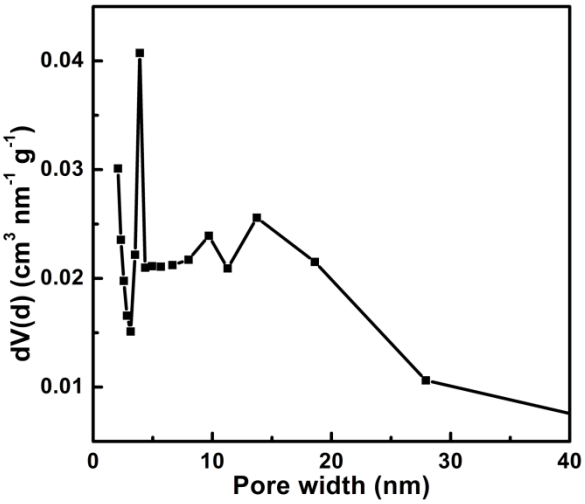

Fig. S5 The pore size distribution calculated by BJH method according to the N_2 sorption isotherm.

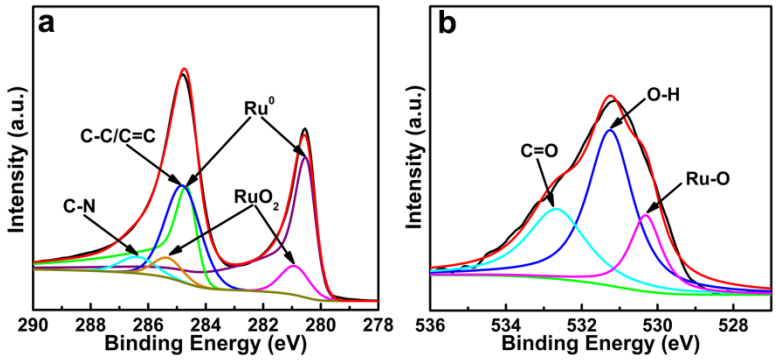

Fig. S6 (a) C 1s + Ru 3d and (b) O 1s XPS spectra of Ru@NCHNSs.

As displayed in the C 1s + Ru 3d spectrum (Fig. S6a), the peaks at 284.8 and 286.4 eV are ascribed to C-C/C=C and C-N. The binding energies at 280.5 and 284.7 eV correspond to Ru $3d_{5/2}$ and Ru $3d_{3/2}$ of metallic Ru. Meanwhile, the other peaks at 280.9 and 285.3 eV are attributed to Ru $3d_{5/2}$ and Ru $3d_{3/2}$ of RuO_2. The high-resolution O1s spectrum is also deconvoluted into three peaks at 530.3 eV (Ru-O), 531.2 eV (O-H), and 532.6 eV (C=O), implying traces of Ru oxide on the surface of the obtained Ru@NCHNSs.

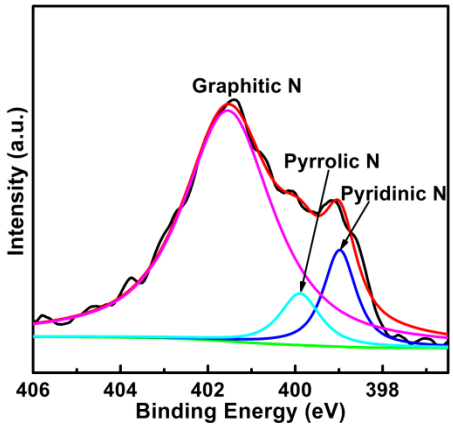

Fig. S7 N1s XPS spectrum of NCHNSs.

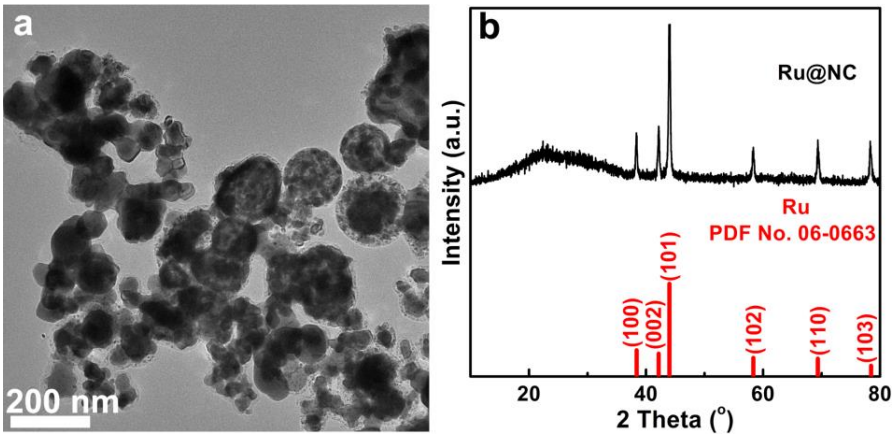

Fig. S8 (a) TEM image and PXRD pattern of Ru@NC.

The morphology and structural characterizations of Ru@NC were studied by TEM and PXRD, shown in Fig. S8. In sharp contrast, it is clear that numerous larger-sized Ru NPs are randomly distributed in the carbon matrix. Consequently, this result undoubtedly proves that the SiO_2 nanosphere as a template plays a crucial role in the fabrication of NCHNS, which contributes to the uniform distribution and excellent stabilization of small-sized Ru NPs.

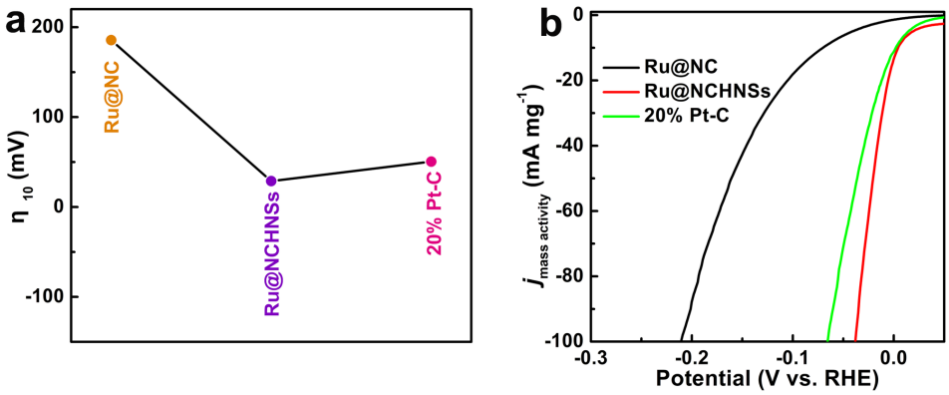

Fig. S9 (a) η_{10} data and (b) calculated mass activity of Ru@NC, Ru@NCHNSs, and 20% Pt-C, respectively.

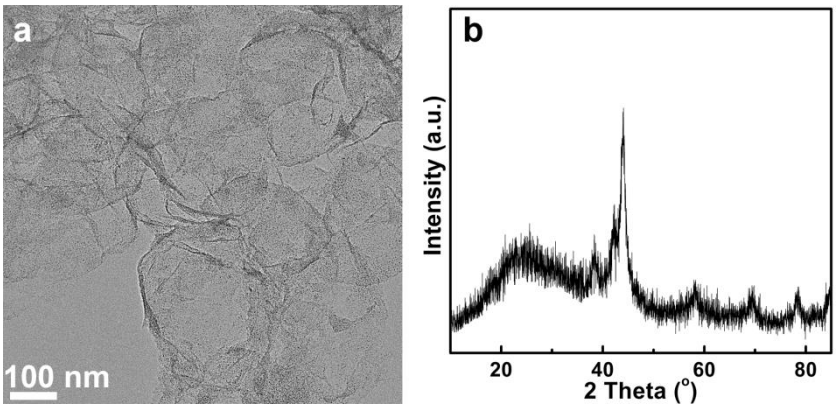

Fig. S10 (a) TEM image and (b) PXRD pattern of Ru@NCHNSs after the stability test.

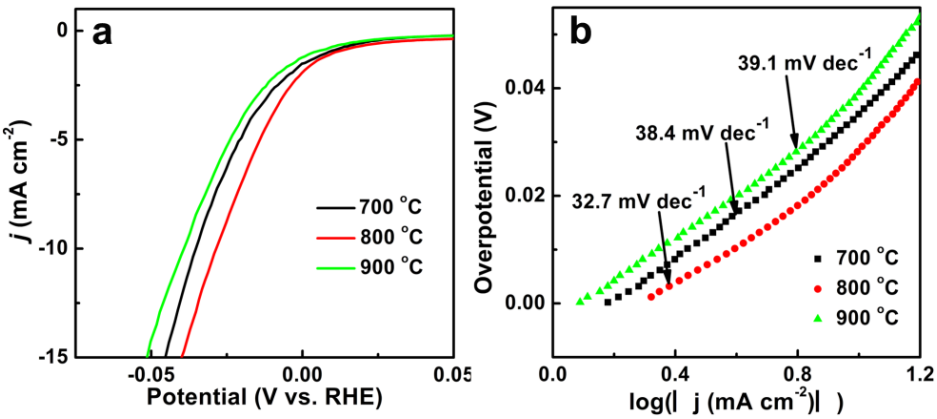

Fig. S11 (a) Polarization curves and (b) corresponding Tafel plots of different catalysts.

In general, the pyrolysis temperature is an important factor for the synthesis of carbon materials. Consequently, the catalytic activities of Ru@NCHNSs obtained at 700, 800, and 900 ^{o}C were systematically pre-investigated. As exhibited in Fig. S11, the hybrid synthesized at 800 ^{o}C presents the lowest overpotential (η_{10}) at the current density of 10 mA cm^{-2}, and the smallest Tafel slope among the three products, implying the best electrocatalytic activity for the HER. Hence, 800 ^{o}C is considered as an ideal pyrolysis temperature in the work.

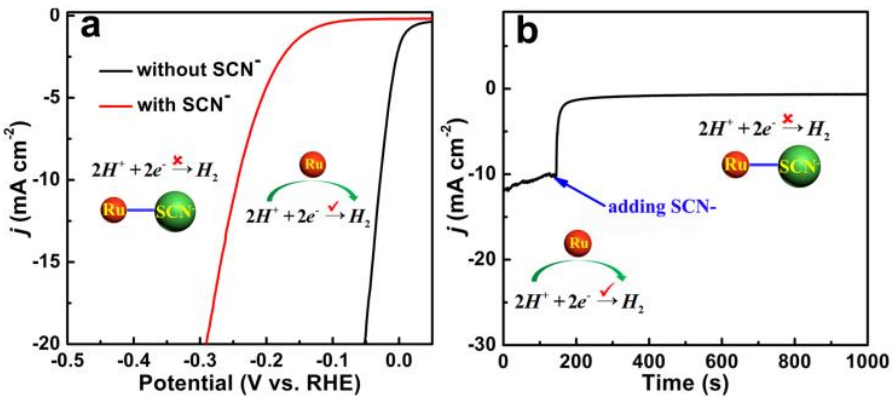

Fig. S12 (a) LSV curves and (b) CA curve of Ru@NCHNSs in N_2-saturated 1.0 M KOH with and without SCN^-. Insets in (a, b) show the pathway for the HER before and after the addition of SCN^-.

To disclose the role of Ru active sites for the HER, potassium thiocyanate (KSCN) was added into N_2-saturated 1.0 M KOH solution, because SCN^- ions are regarded as poisoning species to metal active sites. As expected, the HER activity of Ru@NCHNSs is drastically decreased after adding SCN^- ions into the solution, as proven by the largely negative shift of the onset potential and η_{10} (Fig. S12a). Furthermore, a sharp jump of current density from 10 to 2.05 mA cm^{-2} is obviously seen at t = 200 s in the chronoampherometry (CA) curve (Fig. S12b). Due to the introduction of SCN^-, the Ru sites are attacked and poisoned, further leading to inferior HER activity. As a result, we conclude that Ru NPs should be the active sites of the Ru@NCHNSs catalyst.

S2. Table in Supporting Information

Table S1 Comparison of electrocatalytic HER activity in 1.0 M KOH for Ru@NCHNSs with other HER electrocatalysts.

Catalysts	Tafel slope [mV dec^{-1}]	η_{10} (mV)	Reference
Ru@NCHNSs	**32.7**	**28.8**	**This work**
np-$Cu_{53}Ru_{47}$	30	15	*ACS Energy Lett.* 2020, **5**, 192.
Co_1/PCN	52	89	*Nat. Catal.*, 2019, **2**, 134.
IrP_2@NC	50	28	*Energy Environ. Sci.*, 2019, **12**, 952.
Ru-MoS_2/CC	114	41	*Appl.Catal. B: Environ.*, 2019, **249**, 91.
Ru/C-H_2O/ CH_3CH_2OH	47	53	*Appl.Catal. B: Environ.*, 2019, **258**, 117952.
N-Co_2P/CC	51	34	*ACS Catal.* 2019, **9**, 3744.
Ni_5Co_3Mo-OH	59	52	*ACS Energy Letter.* 2019, **4**, 952.
Ru-NGC	40	65	*Chem. Commun.*, 2019, **55**, 965.
Mo_2C@NC@Pt	57	47	*ACS Appl. Mater. Interfaces*, 2019, **11**, 4047.
Ni_2P-Cu_3P/NiCuC	177	78	*ACS Catal*. 2019, **9**, 6919.
Ni@Ni_2P-Ru HNRs	31	41	*J. Am. Chem. Soc.* 2018, **140**, 2731.
Mo_2N-Mo_2C/HGr	152	154	*Adv. Mater.* 2018, **30**, 1704156.
MoP/CNTs-700	73	86	*Adv. Funct. Mater.*, 2018, **28**, 1706523.
V-doped CoP	67.6	71	*Chem. Sci.*, 2018, **9**, 1970.
Ni_2P@NPCNFs/CC	80	104	*Angew. Chem. Int. Ed.*, 2018, **130**, 1981.